

Spatial filtering using media with indefinite permittivity and permeability tensors

D. Schurig^{a)} and D. R. Smith

University of California, San Diego, San Diego, California 92093

(Received 19 November 2002; accepted 27 January 2003)

Bilayers of media for which the permittivity and permeability tensors are indefinite—that is, not all principle elements possess the same sign—can be used to construct low-, high-, and bandpass spatial filters. These filters possess sharp adjustable roll-offs, and can operate both below and above free-space cutoff to select specific spatial variation components or beam angles from a source or image. © 2003 American Institute of Physics. [DOI: 10.1063/1.1562344]

Recently, there has been much discussion of proposed and implemented media with negative permittivity and permeability.^{1–4} Media with negative electromagnetic properties have not been found in violation of any fundamental physical principles,^{1,5,6} and implementations have been verified both experimentally and with simulation.^{7–10} In this letter, we outline a potentially useful application of these media, spatial filtering.

Electromagnetic spatial filters have seen many applications in the broad categories of *image enhancement* and *information processing*, particularly, but not exclusively, in the optical spectrum. These include spatial spectrum analysis, matched filtering, radar data processing, aerial imaging, industrial quality control, and biomedical applications.^{11,12} A simple, traditional spatial filtering arrangement is shown in Fig. 1(a). Occlusions, Fig. 1(c), placed in the center of the Fourier plane, implement various filter types. A functionally equivalent device can be constructed using appropriate media with negative material properties, Fig. 1(b). The latter has two advantages. First, the spatial filter band edge can be placed beyond the free-space cutoff, i.e., processing of near-field components is possible. The traditional setup can only transmit components that propagate in the medium that surrounds the optical elements. Second, the device is inherently compact. In many cases the device can consist of a bilayer of media that is only a few wavelengths thick. The traditional set up is, typically, at least four focal lengths long, and the focal length is much greater than a wavelength.

While low-pass spatial filters may be implemented with layers of isotropic media, high-pass filters require anisotropy. Specifically, we need media that have permittivity and permeability tensors that are indefinite—not all of their principle components have the same sign.^{13–16} We refer to such media in general as *indefinite media* and the particular subclass of media that has a dispersion relation that implements high-pass filtering as *anticutoff*.

Single layers of isotropic media with a cutoff different from that of free space as well as all *anticutoff* media have poor impedance matching to free space. This means that most incident power is reflected and a useful transmission filter can not be implemented. This situation is mitigated by

forming a *compensating* bilayer. The material properties of one layer can be chosen to be the negative of the other layer. If the layer thicknesses are also equal to each other, the resulting bilayer then matches to free space and has a transmission coefficient that is unity in the pass band of the media itself.¹⁷

To see how to construct media with desired spatial pass bands, we begin by assuming a material whose anisotropic permittivity and permeability tensors are simultaneously diagonalizable, having the form

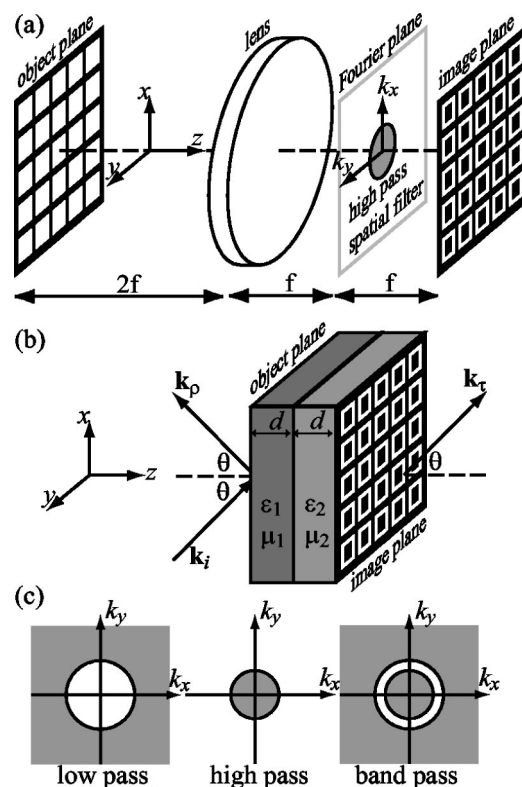


FIG. 1. Traditional (a) and proposed (b) spatial filter configurations. The devices are shown operating as high-pass filters, i.e., edge detectors. Proposed setup (b) is a *compensating* bilayer shown with representative incident, reflected, and transmitted wave vectors. In the traditional configuration, occlusions, (c), are used to implement low-, high-, and bandpass spatial filters. This functionality is available with both configurations.

^{a)}Electronic mail: dschurig@ucsd.edu

$$\boldsymbol{\epsilon} = \begin{pmatrix} \epsilon_x & 0 & 0 \\ 0 & \epsilon_y & 0 \\ 0 & 0 & \epsilon_z \end{pmatrix}, \quad \boldsymbol{\mu} = \begin{pmatrix} \mu_x & 0 & 0 \\ 0 & \mu_y & 0 \\ 0 & 0 & \mu_z \end{pmatrix}. \quad (1)$$

We will consider layered media with surfaces normal to one of the principle axes, which we define to be the z axis. We demonstrate our analysis using a plane wave with the electric field polarized along the y axis, though it is generally possible to construct media that are polarization independent, or exhibit different classes of behavior for different polarizations:

$$\mathbf{E} = \hat{\mathbf{y}} e^{i(k_x x + k_z z - \omega t)}. \quad (2)$$

Plane-wave solutions to Maxwell's equations with this polarization have $k_y = 0$ and satisfy

$$k_z^2 = \epsilon_y \mu_x k_0^2 - \frac{\mu_x}{\mu_z} k_x^2, \quad (3)$$

where $k_0 = \omega/c$ and the material parameters are relative to free space. Since we have no x or y oriented boundaries or interfaces, nonoscillatory solutions, which result in field divergence when unbounded, are not allowed in those directions. Thus, k_x is restricted to be real. Also, since k_x represents a variation transverse to the surfaces of our layered media, it is conserved across the layers, and naturally parametrizes the solutions.

In the absence of losses, the sign of k_z^2 can be used to distinguish the nature of the plane-wave solutions. $k_z^2 > 0$ corresponds to real valued k_z and propagating solutions. $k_z^2 < 0$ corresponds to imaginary k_z and exponentially growing or decaying (evanescent) solutions. When $\epsilon_y \mu_z > 0$, there will be a value of k_x for which $k_z^2 = 0$. This value, which we denote k_c , is the cutoff wave vector separating propagating from evanescent solutions. From Eq. (3) this value is $k_c = k_0 \sqrt{\epsilon_y \mu_z}$. For spatial filtering we will use the following dispersion classes:

$$\text{cutoff } \epsilon_y \mu_x > 0 \text{ and } \mu_x / \mu_z > 0,$$

$$\text{anticutoff } \epsilon_y \mu_x < 0 \text{ and } \mu_x / \mu_z < 0.$$

A *cutoff* medium supports propagating solutions for $k_x < k_c$, and evanescent solutions for $k_x > k_c$. Examples of this medium class include free space, and any medium with $\boldsymbol{\epsilon}$ and $\boldsymbol{\mu}$ tensors both positive or both negative definite. An *anticutoff* medium requires indefinite material property tensors, characterized by single sheeted hyperbolic dispersion.¹⁴ The *anticutoff* medium supports propagating solutions for $k_x > k_c$, and evanescent solutions for $k_x < k_c$. Figure 2 shows both classes of dispersion, for several different values of the cutoff wave vector, k_c .

Each of the dispersion classes, *cutoff* and *anticutoff*, can be further categorized into two subtypes, distinguished by the directions of the group velocity. The group velocity which is the gradient of the dispersion relation, $\mathbf{v}_g \equiv \nabla_{\mathbf{k}} \omega(\mathbf{k})$, must lie normal to the dispersion relation's constant frequency surfaces. One can switch types by negating both the $\boldsymbol{\mu}$ and $\boldsymbol{\epsilon}$ tensors.

To describe the material properties of the layered filters introduced here, we find it convenient to define the following two basis matrices:

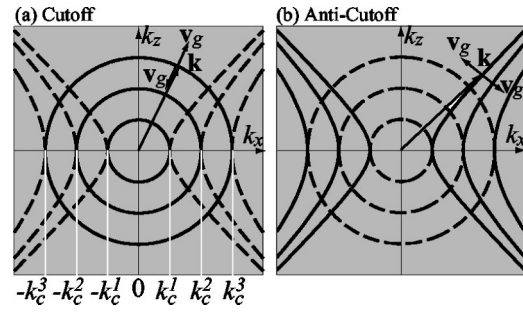


FIG. 2. Dispersion curves for (a) *cutoff* and (b) *anticutoff* media for several different values of the cutoff, k_c . Solid lines indicate real valued k_z , and dashed lines indicate imaginary values. A wave vector, \mathbf{k} , is shown, and both possible group velocity directions associated with that wave vector.

$$\boldsymbol{\sigma}_0 = \begin{pmatrix} 1 & 0 & 0 \\ 0 & 1 & 0 \\ 0 & 0 & 1 \end{pmatrix}, \quad \boldsymbol{\sigma}_1 = \begin{pmatrix} 1 & 0 & 0 \\ 0 & 1 & 0 \\ 0 & 0 & -1 \end{pmatrix}. \quad (4)$$

The first is the identity matrix and the second is an indefinite matrix, both of which are isotropic in the x - y plane. Though the discussion of dispersion above employed a specific polarization orientation—with an x - z plane of incidence—the devices discussed here will work equally well with an y - z plane of incidence, or any angle in between.

Low-pass filtering only requires isotropic media. The material properties of the two layers of the *compensating* bilayer are written explicitly in terms of the cutoff wave vector, k_c .

$$\boldsymbol{\epsilon}_1 = \boldsymbol{\mu}_1 = \frac{k_c}{k_0} \boldsymbol{\sigma}_0 + i \gamma \boldsymbol{\sigma}_0$$

and

$$\boldsymbol{\epsilon}_2 = \boldsymbol{\mu}_2 = -\frac{k_c}{k_0} \boldsymbol{\sigma}_0 + i \gamma \boldsymbol{\sigma}_0. \quad (5)$$

$\gamma \ll 1$ is the parameter that introduces absorptive loss. The cutoff, k_c , determines the upper limit of the pass band. Note that $\boldsymbol{\epsilon} = \boldsymbol{\mu}$ for both layers, so this device will be polarization independent. Adjusting the loss parameter, γ , and the layer thickness controls the filter roll off characteristics.

High-pass filtering requires indefinite material property tensors:

$$\boldsymbol{\epsilon}_1 = \boldsymbol{\mu}_2 = \frac{k_c}{k_0} \boldsymbol{\sigma}_1 + i \gamma \boldsymbol{\sigma}_0$$

and

$$\boldsymbol{\epsilon}_2 = \boldsymbol{\mu}_1 = -\frac{k_c}{k_0} \boldsymbol{\sigma}_1 + i \gamma \boldsymbol{\sigma}_0. \quad (6)$$

Here, the cutoff wave vector, k_c , determines the lower limit of the pass band. With $\boldsymbol{\epsilon} \approx -\boldsymbol{\mu}$ for both layers, this device will be *externally* polarization independent.

The transmission coefficient, τ , and the reflection coefficient, ρ , can be calculated using standard transfer matrix techniques. We show these coefficients for several low-, and high-pass filters with various cutoffs in the free-space propagating range, $k_c < k_0$, Fig. 3(a), and in range beyond cutoff, $k_c > k_0$, Fig. 3(b). The independent variable is given as an angle, $\theta = \sin^{-1}(k_x/k_0)$, in Fig 3(a), since in this range the

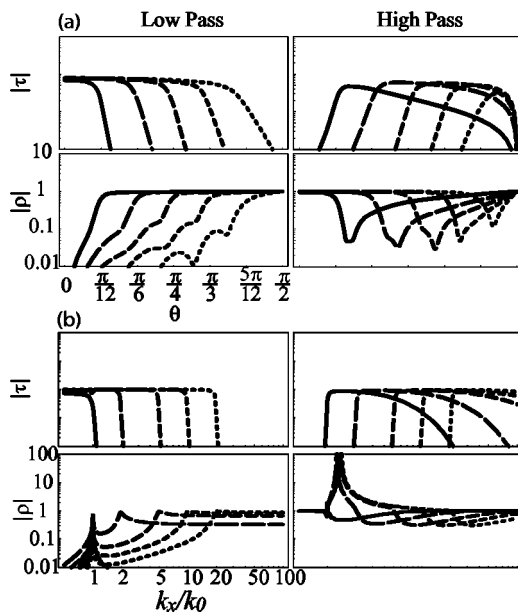


FIG. 3. Reflection and transmission coefficients vs transverse wave vector for low- and high-pass filters. In (a), the filter band edges are below the free-space cutoff, k_0 . The values for $\theta_c \equiv \sin^{-1}(k_c/k_0)$ are $\pi/12$, $\pi/6$, $\pi/4$, $\pi/3$ and $5\pi/12$ from solid to shortest dashed lines, respectively, $k_0d = 4\pi$ except for $\theta_c \equiv \pi/12$ where $k_0d = 6\pi$. In (b), the filter band edges are at or above the free space cutoff, k_0 . The values for k_c/k_0 are 1,2,5,10,20 from solid to shortest dashed lines respectively, $k_0d = 4\pi$. For all filters, $\gamma = 0.01$.

incident plane waves propagate in real directions. For incident propagating waves, $k_x/k_0 < 1$ and $0 < \theta < \pi/2$, the reflection and transmission coefficients must, and do obey, $|\rho|^2 + |\tau|^2 \leq 1$, to conserve energy. Incident evanescent waves, $k_x/k_0 > 1$ do not transport energy, so no such restriction applies.

Figure 4 shows the field intensity pattern for several Gaussian beams incident on a band pass filter with cutoffs in the propagating range. This multilayer structure transmits beams that are in a midangle range and reflects beams that are small and large angle incident. This device is unusual in two ways. Standard materials cannot reflect normally incident beams and transmit higher angle ones. Also, though an upper critical angle is not unusual, it can only occur when a beam is incident from a higher-index media to a lower-index media, and not for a beam incident from free space, as it is in Fig. 4. The action of the compensating layers also permits a greater transmittance with less distortion than is possible with any single layer of normal materials.

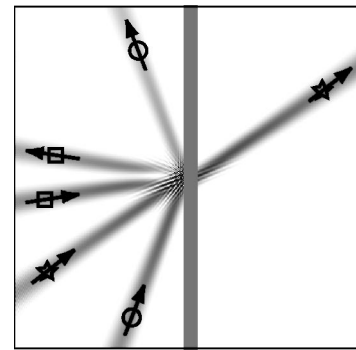


FIG. 4. Reflection and transmission of Gaussian beams incident on a bandpass filter. The bandpass filter has $\theta_c = 24^\circ$ and 58° , $k_0d = 4\pi$, and $\gamma = 0.01$. The beams have width $10\lambda_0$ and incident angles 9° (squares), 34° (stars), and 69° (circles). The scale on the transmission side is compressed to compensate for the attenuation of the beam.

We have shown how media with negative electromagnetic property tensor elements can be used to construct high-, low-, and bandpass spatial filters with cutoffs tunable both above and below the free-space cutoff wave vector. The far-field filters are particularly flexible and can be used either in transmission or reflection.

This work was supported by DARPA through grants from ONR (Contract No. N00014-00-1-0632) and AFOSR (Contract No. 972-01-2-0016).

¹V. G. Veselago, *Sov. Phys. Usp.* **10**, 509 (1968).
²D. R. Smith, W. Padilla, D. C. Vier, S. C. Nemat-Nasser, and S. Schultz, *Phys. Rev. Lett.* **84**, 4184 (2000).
³J. B. Pendry, A. J. Holden, W. J. Stewart, and I. Youngs, *Phys. Rev. Lett.* **76**, 4773 (1996).
⁴J. B. Pendry, A. J. Holden, D. Robbins, and W. J. Stewart, *IEEE Trans. Microwave Theory Tech.* **47**, 2075 (1999).
⁵D. R. Smith and N. Kroll, *Phys. Rev. Lett.* **85**, 3966 (2000).
⁶F. D. M. Haldane, e-print (2002), cond-mat/0206420.
⁷R. A. Shelby, D. R. Smith, and S. Schultz, *Science* **292**, 79 (2001).
⁸P. Markos and C. M. Soukoulis, *Phys. Rev. E* **65**, 036622 (2002).
⁹F. J. Rachford, D. L. Smith, P. F. Loschialpo, and D. W. Forester, *Phys. Rev. E* **66**, 036613 (2002).
¹⁰C. Caloz, C.-C. Chang, and T. Itoh, *J. Appl. Phys.* **90**, 5483 (2001).
¹¹J. W. Goodman, *Introduction to Fourier Optics* (McGraw-Hill, New York, 1988), chap. 7.
¹²S. P. Almeida and G. Indebetouw, *Applications of Optical Fourier Transforms* (Academic, New York, 1982), chap. 2.
¹³D. R. Smith and D. Schurig, *Phys. Rev. Lett.* **90**, 077405 (2003).
¹⁴I. V. Lindell, S. A. Tretyakov, K. I. Nikoskinen, and S. Ilvonen, *Micro-wave Opt. Technol. Lett.* **31**, 129 (2001).
¹⁵K. G. Balmain, A. A. E. Lutgen, and P. C. Kremer, *IEEE Antennas and Wireless Propagation Letters* **1**, 146 (2002).
¹⁶K. Balmain (private communication).
¹⁷A. Lakhtakia, *Int. J. Infrared Millim. Waves* **23**, 339 (2002).